

## Electronic supplementary information

# A robust epoxy nanocomposite with iron oxide decorated cellulose nanofiber as a sustained drug delivery vehicle for an antibacterial drug

Nobomi Borah,<sup>a</sup> Muzamil Ahmad Rather,<sup>b</sup> Bibrita Bhar,<sup>c</sup> Biman B. Mandal,<sup>c,d,e</sup> Manabendra Mandal,<sup>b</sup> Niranjana Karak<sup>\*a</sup>

<sup>a</sup>Advanced Polymer and Nanomaterial Laboratory (APNL), Department of Chemical Sciences, Tezpur University, Napam, 784028, Tezpur, Assam, India.

<sup>b</sup>Department of Molecular Biology and Biotechnology, Tezpur University, Napaam, Tezpur, 784028, Assam, India

<sup>c</sup>Biomaterials and Tissue Engineering Laboratory, Department of Biosciences & Bioengineering, Indian Institute of Technology Guwahati, Guwahati – 781039, Assam, India

<sup>d</sup>Centre for Nanotechnology, Indian Institute of Technology Guwahati, Guwahati – 781039, Assam, India

<sup>e</sup>Jyoti and Bhupat Mehta School of Health Sciences and Technology, Indian Institute of Technology Guwahati, Guwahati – 781039, Assam, India

**\*Corresponding author, E-mail:** karakniranjan@gmail.com, **Telephone:** +91 3712-267009

## ESI.1 Materials and methods

### ESI.1.1 Preparation of epoxy resin (TAE)

The TAE was obtained as reported in our previous work.<sup>1</sup> To state concisely, 5.0 g TA was mixed with 11.1 mL epichlorohydrin in a round bottom flask. When a reaction temperature of 65 °C was attained, 14.3 mL of 5 N NaOH was added dropwise for initiating the epoxidation reaction. After the addition was completed, the reaction temperature was raised to 80 °C, and

the stirring was continued for another 1 h. The resultant viscous mass upon cooling was washed successively with brine solution and freshwater followed by dissolving in THF. On evaporating the solvent, resinous product TAE was obtained.

### **ESI.1.2 Instrumentations**

The nanostructure and morphology of the prepared nanohybrid IONP@CNF and nanocomposites were identified using a scanning electron microscope (SEM) (Model JOEL JSM-6390LV, Japan), field emission scanning electron microscope (FESEM, Model JOEL, Japan) and a transmission electron microscope (TEM) (Model TECNAI, G2 20 S-TWIN, USA). The chemical structure and bonding interactions present in CNFs, IONP@CNFs, and nanocomposites were investigated by a Nicolet Fourier Transform InfraRed (FTIR) spectrophotometer (Impact 410, USA), X-ray photoelectron spectrometer (Model ESCALAB Xi+, Thermo Fisher Scientific Pvt ltd, UK). The studies of the composition and crystal structure of the samples were conducted in a Bruker XS X-ray diffractometer (D8 FOCUS, Germany) using a Copper  $K\alpha$  beam. The absorption spectra of the nanohybrids were recorded in a Thermo Scientific's Evolution 300 UV-spectrophotometer (USA). A thermogravimetric instrument (TGA) of Perkin Elmer (TGA 4000, USA) was used for analyzing the thermal properties of the samples under an inert atmosphere of  $N_2$  operating at a temperature range of 30-600 °C with a heating rate 10 °C per min. The mechanical performance of the nanocomposite was measured according to the ASTM D 638 standard in a Universal Testing Machine (UTM) (WDW-10, JINAN, China) with a load cell 0.5 kN at a strain rate of 5 mm  $min^{-1}$ , while the scratch hardness was measured in an automatic scratch tester (Sheen, UK). The impact strengths of the nanocomposites were evaluated using a manual impact tester (S.C. Dey & Co., India) by the standard falling ball method with a ball of 0.85 kg and a maximum distance of 100 cm.

### **ESI.1.2 Determination of total phenolic content**

The presence of total phenolic content in the tea extract was determined using the Folin-Ciocalteu reagent by following the Singleton procedure.<sup>2</sup> Initially, to a 0.3 mL diluted TE, 2.7 mL of ten times diluted Folin-Ciocalteu reagent was added and mixed properly. To this solution, 2 mL of 7.5% sodium carbonate solution was added followed by incubating the mixture for 15 min in dark. Afterwards the absorbance of the sample was recorded at 760 nm. The standard curve was plotted using five known concentrations of gallic acid (from 40 mg/L to 200 mg/L) and from this curve, the total phenolic content of TE was evaluated in mg gallic acid equivalent (GAE) per g of WTF.

### **ESI.1.3 Hemolytic activity study**

The method described by Rather et al. (2022) was followed to investigate the hemolytic activity of IO@CNF1.0/TAE nanocomposite at different concentrations (1 mg, 5 mg, and 10 mg, in duplicates).<sup>3</sup> Firstly, 40 mL Defibrinated Sheep Blood (ThermoFisher Scientific) was centrifuged at 10,000 rpm for 15 min at 4°C. The supernatant was discarded, and the pellet was washed with 0.9% NaCl solution and centrifuged again at 10,000 rpm for 15 min at 4°C. The washing was repeated two times and the final pellet was suspended in 0.9% NaCl. Then, RBC suspension was pipetted in different centrifuge tubes. Finally, samples were added to centrifuge tubes to make the final concentration of 50, 100, 150, and 200 µg/mL. The reaction mixture was placed at 37°C for 30 min and centrifuged at 10,000 for 5 min. Then, 200 µl supernatant from each centrifuge tube was poured into a 96-well plate and the optical density (OD) was measured at 540 nm (Thermo Scientific Multiscan GO) to quantify cell lysis and release of hemoglobin. Triton-X and water were used as positive controls (PC), while the centrifuge tube with RBC suspension in 0.9% NaCl served as negative control (NC). The percent hemolysis was calculated as follows.

$$\text{Hemolysis (\%)} = [(AB_S - AB_{NC}) / (AB_{PC} - AB_{NC})] \times 100 \quad (1)$$

Where  $AB_{PC}$  is the absorbance of positive control,  $AB_{NC}$  is the absorbance of negative control, and  $AB_S$  is the absorbance of treated samples.

#### **ESI.1.4 Ampicillin (AC) loading in the nanocomposites**

In order to encapsulate AC into the resinous nanocomposite, the drug was dissolved in 100  $\mu$ L water and to this mixture, the required amount of IONP@CNF dispersion was added with magnetic stirring for 1 h. Then this drug-loaded IONP@CNF was added to TAE and finally stirred at 70 °C for 30 min to obtain the nanocomposite. The thermosets were then prepared by mixing with the hardener and cured at room temperature (RT) for 3 days. The thermosets were then washed with water to remove any loosely adhered AC and the aliquot was measured for any traces of AC using UV-visible spectrophotometer at 227 nm wavelength against a standard AC concentration curve. From the amount of AC leached out, the encapsulation efficiency was calculated using the following equation.

$$\text{Encapsulation efficiency (\%)} = [(M_0 - M_r) / M_0] \times 100 \quad (2)$$

Where  $M_0$  and  $M_r$  are the amount of drug initially added and leached out during washing from the thermoset, respectively.

#### **ESI.1.5 AC release and kinetic study**

The AC release rates from the nanocomposite thermosets were studied in phosphate buffer saline (PBS) at 37 °C for a period of 5-7 days. For each composition, a definite amount of thermoset was cut to small pieces, immersed in 100 mL PBS solution, and placed in an incubator shaker at a temperature of 37 °C. Aliquots were taken from the solution at particular time intervals and replaced with fresh PBS solution to maintain a constant volume. The absorbance of these aliquots was measured in a UV-visible spectrophotometer at 227 nm wavelength from which the amount of AC released was calculated with the assistance of the

standard curve. The process was repeated thrice. In order to calculate the cumulative drug release rate, the following equation was utilized.

$$\text{Cumulative release (\%)} = (M_t/M_0) \times 100 \quad (3)$$

Similarly, the kinetics of drug release was studied using four different models namely, zero order, first order, Korsmeyer-Peppas model, and Higuchi model as shown in Table SI.1, equations (4) - (7).<sup>5</sup> The best-supported model was evaluated using the curve fitting method and the correlation coefficient values corresponding to each model.

Model	Equation	Graph axes	Equation No.
Zero order	$M_t = K_0t + M_e$	Cumulative release vs time	4
First order	$\log (M_e - M_t) = -(K_1/2.303)t + \log M_0$	Log cumulative release vs time	5
Korsmeyer-Peppas	$M_t/M_e = K_m(t)^n$	Log cumulative release vs time	6
Higuchi	$M_t = K_H (t)^{1/2}$	Cumulative release vs (time) <sup>1/2</sup>	7

**Table ESI.1:** Kinetic models with equations utilized for studying the drug release mechanism

### ESI.1.6 Antimicrobial activity of films by disc diffusion assay

The antimicrobial activity of films against both Gram-positive and Gram-negative pathogenic bacteria was determined using the agar diffusion method.<sup>4</sup> Bacterial cultures of different bacterial species (*SA*, *SP*, *YE*, and *KP*) were grown overnight in Luria Broth (LB). The OD at 600 nm of the fresh cultures was set at 0.4 which was used in the experiment. The cultures (100  $\mu$ L) were spread on the prepared Luria-Bertani agar (LBA) plates. The films

were placed onto the agar plates and incubated overnight at 37°C for 24 h. After incubation, the plates were evaluated for antimicrobial activity and the zone of inhibition (ZOI) was measured accordingly.

### **ESI.1.7 Biodegradation study**

The McFarland turbidity method was employed for studying the accelerated biodegradation of the nanocomposite thermosets (without any drug) using the *Bacillus subtilis* (*B. subtilis*) bacterial strain.<sup>1</sup> A nutrient medium was prepared using 100 mL deionized water and 2.5 g of LB nutrient broth and the mixture was sterilized in an autoclave at 120 °C under 15 lb pressure for 30 min. The culturing of the bacterial strain was carried out in an incubator for 48 h at 30 °C by adding 100 µL aliquots of the strain into the above mixture. Subsequently, the thermosets, previously sterilized under UV light exposure, were placed in 15 mL centrifuge tubes and 1 mL of the cultured media was added to each tube, while the volume was increased to 10 mL by adding the sterilized nutrient medium. The tubes were then placed in an incubator shaker at 37 °C and their OD values were measured in a UV-visible spectrophotometer (in terms of absorbance) periodically for monitoring the growth of the bacteria. After completion of the test, the thermosets were taken out, washed with ethanol, and subject to weight measurements. The weight loss percentages were then calculated using the equation as given below.

$$\text{Weight loss (\%)} = [(W_i - W_f)/W_i] \times 100 \quad (8)$$

Where  $W_i$  and  $W_f$  are the initial and final weights, respectively of the nanocomposite thermosets.

### **ESI.1.8 *In vitro* biocompatibility assessment**

Biocompatibility assessment of the fabricated nanocomposites and TAE thermosets was conducted using human dermal fibroblasts (HDF) via the live-dead assay. The cells were

procured from Himedia, India, and cultured in high glucose DMEM (Gibco; Thermo Fisher Scientific, USA) containing 10% fetal bovine serum (FBS, Gibco; Thermo Fisher Scientific, USA) and 1X antibiotic-antimycotic solution (Himedia, India). The films (5×5 mm<sup>2</sup>) were sterilized using (70% v/v) for 10 min, rinsed with PBS, and preconditioned in media for 24 h. HDF cells were trypsinized when they reached 70-80% confluence and seeded (~2×10<sup>4</sup> cells on each) on the films and tissue culture plate (TCP). TCP was considered as the control surface for comparison. The seeded cells were assessed using live-dead (Sigma-Aldrich, USA) reagents on day 1 and day 7 after seeding. At first, the cell-seeded films and TCP were gently washed with PBS and incubated with a solution containing 4 μM calcein-AM (stains adherent live cells and shows green fluorescence) and 2 μM ethidium homodimer (stains dead cells and shows red fluorescence) for 15 min 37 °C in humidified incubator.<sup>6</sup> After staining, the samples were washed with PBS and were imaged using a fluorescent microscope (ZEISS Axio Observer, Germany) and representative images were presented.

#### **ESI.1.9. UV-blocking**

The UV blocking percentages can be measured using a UV-visible spectrometer and recording the transmittance of the thermosets in the 200-400 nm range. The blocking percentages for both UV-A and UV-B regions can be calculated using the following equations:

$$\text{UV-A blocking (\%)} = 100 - T_{315-400} \quad (9)$$

$$\text{UV-A blocking (\%)} = 100 - T_{280-315} \quad (10)$$

Where  $T_{315-400}$  is the average transmittance of the thermoset in the 315 to 400 nm region (i.e., UV-A region) and  $T_{280-315}$  is the average transmittance in the range of 280-315 nm, corresponding to the UV-B region.<sup>7</sup>

#### **ESI.1.10. Water absorption and gel content**

The water absorption behavior of the thermosets was studied in PBS saline solution at RT. For the same, initially weighted thermosets were immersed in PBS solution and their weight gain was measured by periodically removing the thermosets from the medium, wiping with a tissue, and measuring their weight. The weight gain percentage was then calculated using the below-mentioned equation:

$$\text{Weight gain (\%)} = [W_t - W_i] / W_i \times 100 \quad (11)$$

Where  $W_i$  is the initial weight of the thermoset and  $W_t$  is its weight after immersing in PBS medium for time  $t$ .<sup>8</sup>

## **ESI.2 Result and Discussion**

### **ESI.2.1 Characterization of the nanohybrid**

The EDX spectrum of IONP@CNFs as displayed in Fig. SI.1(a) revealed the presence of iron in the IONP@CNFs surfaces which was evidenced by the elemental mapping images for carbon, oxygen, and iron as shown in Fig.SI.1(b), SI.1(c), and SI.1(d), respectively.



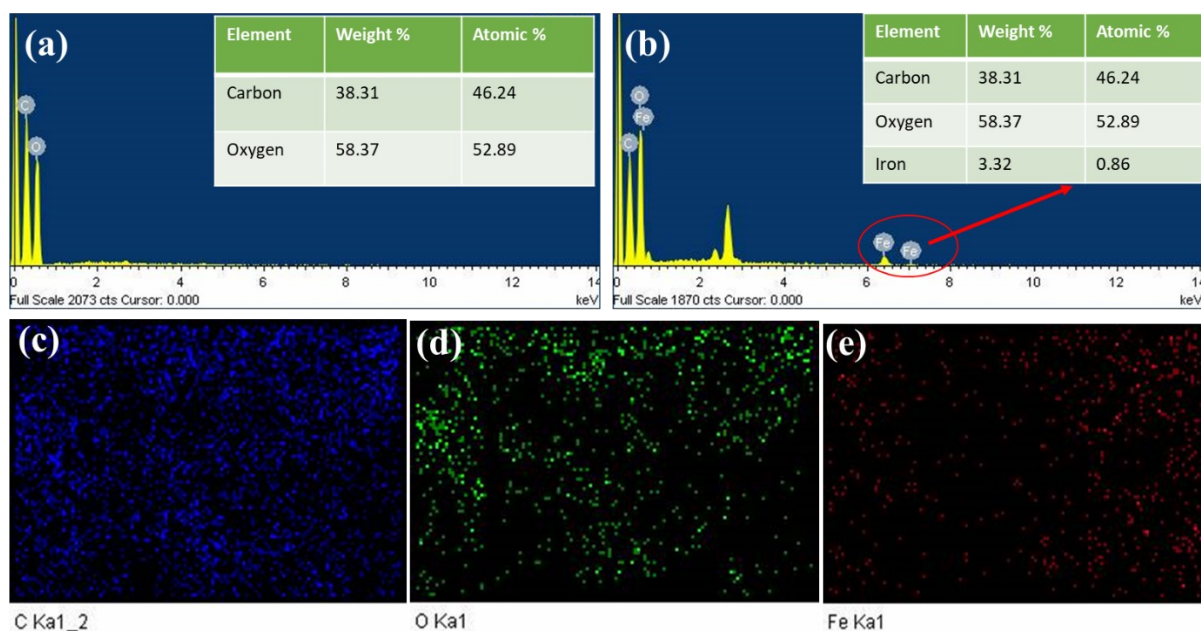


**Fig. ESI.1:** EDX spectrum of (a) CNFs and (b) IONP@CNFs with inset atomic wt%, showing the presence of iron on IONP@CNFs along with carbon and oxygen, respective elemental mapping images for (c) carbon, (d) oxygen, and (e) iron.

### ESI.2.2 Characterization of the nanocomposites

Parameters	CNF	IONP @CNF	TAE	IO@CNF 0.25/TAE	IO@CNF 0.50/TAE	IO@CNF 1.00/TAE
T <sub>ON</sub> (°C)	240	209	247	242	241	241
1 <sup>st</sup> stage degradation peak temperature (°C)	331	284	299	300	299	300
2 <sup>nd</sup> stage degradation peak temperature (°C)	-	-	440	450	445	455
Weight residue at 600 (%)	14.1	30.7	29.5	27.1	28.8	30.6
Glass transition temperature, T <sub>g</sub> (°C)	-	-	54	64	66	72

**Table ESI.2:** Different parameters obtained from the thermal study

### ESI.2.3 Kinetics study

**Table ESI. 3:** Kinetic parameters obtained for IO@CNF1.00/TAE at three different pH environments

pH	Korsmeyer Peppas Power law			Zero order		Pseudo-first order		Higushi square root law	
	R <sup>2</sup>	K <sub>m</sub>	n	R <sup>2</sup>	K <sub>0</sub>	R <sup>2</sup>	K <sub>1</sub>	R <sup>2</sup>	K <sub>H</sub>
pH 3.4	0.97	0.41	0.24	0.61	0.097	0.93	0.07	0.68	0.45
pH 7.4	0.89	0.27	0.44	0.96	0.35	0.95	0.06	0.96	0.129
pH 10.4	0.89	0.18	0.23	0.82	0.21	0.87	0.05	0.88	0.99

### ESI.2.4 Antibacterial study of the drug loaded nanocomposites

**Table ESI. 4:** ZOI values of the antibacterial study obtained for the pure and drug loaded thermosets

### References

Bacterial strain	ZOI of TAE thermosets (mm)	ZOI of IO@CNF0.25/TA E thermosets (mm)	ZOI of IO@CNF0.5/TA E thermosets (mm)	ZOI of IO@CNF1.0/TA E thermosets (mm)
SA	12	25	23	31
YE	0	17	15	21
KP	0	19	16	20
ST	0	0	0	12

1. N. Borah, and N. Karak, Tannic acid based bio-based epoxy thermosets: Evaluation of thermal, mechanical, and biodegradable behaviours. *J. Appl. Polym. Sci.*, 2022, **139**, 51792.
2. J. Hassanzadeh, H. A. Al Lawati, and I. Al Lawati, *Anal. Chem.*, 2019, **91**, 10631-10639.
3. M. A. Rather, P. J. Deori, K. Gupta, N. Daimary, D. Deka, A. Qureshi, T. K. Dutta, S. N. Joarder and M. Mandal, *Chemosphere*, 2022, **300**, 134497.
4. D. Sarmah, M. A. Rather, A. Sarkar, M. Mandal, K. Sankaranarayanan, and N. Karak, *Int. J. Biol. Macromol.*, 2023, **237**, 124206.
5. S. A. Chime, G. C. Onunkwo, and I. I. Onyishi, *Res. J. Pharm. Biol. Chem. Sci.*, 2013, **4**, 97-103.
6. B. Bhar, B. Chakraborty, S. K. Nandi, B. and B. Mandal, *Int. J. Biol. Macromol.*, 2022, **203**, 623-637.
7. S. Guzman-Puyol, J. Hierrezuelo, J. J. Benítez, G. Tedeschi, J. M. Porrás-Vázquez, A. Heredia, A. Athanassiou, D. Romero, and J. A. Heredia-Guerrero. *Int. J. Biol. Macromol.*, 2022, **209**, 1985-1994.
8. D. M. Patil, G. A. Phalak, and S. T. Mhaske, *J. Coat. Technol. Res.*, 2017, **14**, 355-365.